Abdominal Imaging

© Springer Science+Business Media New York 2014

Abdom Imaging (2014)
DOI: 10.1007/s00261-014-0183-0

Alveolar echinococcosis: correlation between hepatic MRI findings and FDG-PET/CT metabolic activity

Amel Azizi,[1] Oleg Blagosklonov,[2,3] Ahmed Lounis,[1] Louis Berthet,[2] Dominique-Angèle Vuitton,[4] Solange Bresson-Hadni,[4] Eric Delabrousse[1,3]

[1]Department of Radiology, University Hospital, 3 Boulevard Fleming, 25030 Besançon, France
[2]Departmentof Nuclear Medicine, University Hospital, 3 Boulevard Fleming, 25030 Besançon, France
[3]EA 4662 Nanomedicine Lab, Imagery and Therapeutics, University of Franche-Comté, Besançon, France
[4]WHO Collaborating Centre for Prevention and Treatment of Human Echinococcosis, Besançon, France

Abstract

Objective: To correlate the appearance of alveolar echinococcosis (AE) hepatic lesions in magnetic resonance imaging (MRI) as defined by Kodama, to the metabolic activity visualized in 18-fluoro-deoxyglucose positron emission tomography combined with computed tomography (PET/CT).

Materials and methods: Forty-two patients diagnosed with AE and who underwent both MRI and PET/CT were included. The forty-two hepatic lesions were divided into five types according to Kodama's classification by three independent readers blinded with regard to the PET/CT information. Concerning PET/CT, two independent readers, unaware of the MRI information, considered the results as positive when an increased FDG-uptake was observed at 1 or 3 h after FDG-injection, and as negative when no increased uptake was noted. Inter-observer agreement was assessed by using κ statistics.

Results: Forty-two lesions were counted and the mean diameter of overall evaluated lesions was 6.3 cm. One lesion (2.4%) was categorized as type 1, 11 (26.2%) as type 2, 24 (57.1%) as type 3, 3 (7.1%) as type 4, and 3 (7.1%) as type 5. The inter-observer analysis found a κ coefficient of 0.96. All type-1, 90.9% of type-2 and 87.5% of type-3 lesions showed an increased FDG-uptake on PET/CT images. All non-microcystic AE liver lesions (types 4 and 5) showed no abnormal increased FDG-uptake on PET/CT images. The inter-observer analysis at 1 and 3 h found a κ coefficient of 0.95 and 0.92, respectively.

Conclusions: In patients with AE liver lesions, the absence of microcysts on MRI is strongly correlated to a metabolically inactive disease.

Key words: Alveolar echinococcosis—Liver—MRI—FDG-PET/CT—Metabolic activity

Alveolar echinococcosis (AE) is a rare disease caused by the intrahepatic development of the larvae of the *Echinococcus multilocularis* tapeworm. This parasite, transmitted to humans by ingestion of eggs present in the feces of carnivores, only affects countries in he Northern Hemisphere, such as North America (the upper Midwest region of the United States, Alaska, and Northern Canada), Central-Western Europe, Eastern Russia, Turkey, Japan, and Western China [1, 2].

Despite its parasitic nature, AE behaves like a slow growing liver cancer that can spread to other organs; 90%–100% mortality is observed after 10 years [3], if no treatment is provided. Usually diagnosed at an inoperable stage, AE requires long-term oral treatment by benzimidazoles (BZM), the sole therapy that allows a significant improvement in patient survival [4] by stopping parasite growth [5]. BZM have only a parasitostatic effect on *E. multilocularis*, and furthermore, treatment withdrawal (i.e., in patients with positive PET/CT findings) has been responsible for relapses. Somehow, a parasitocidal effect has been highlighted which implies that discontinuation of treatment is still possible [6, 7].

The major goal of clinicians is thus to determine the appropriate timing for BZM withdrawal in order to reduce its serious side effects and also healthcare costs.

Correspondence to: Eric Delabrousse; *email:* edelabrousse@chu-besancon.fr

Published online: 27 June 2014

Therapeutic efficacy in AE is mainly judged on the basis of repeated imaging evaluation using 18-fluorodeoxyglucose positron emission tomography combined with computed tomography (PET/CT), a valuable, but expensive and irradiant technique in nuclear medicine for detecting disease metabolic activity [8, 9]. It has been shown that delayed PET/CT acquisition (3 h after FDG-injection) provides a better sensitivity in detecting active AE lesions [10] and patients with negative PET/CT findings can safely benefit from treatment discontinuation [5].

Morphological imaging has an important role, not only in the screening and diagnosis of patients but also in their follow-up. Ultrasound is the current method of choice for the screening and monitoring of patients, systematically complemented by a CT-scan study [11–13].

Magnetic resonance imaging (MRI), on the other hand, is not only the best examination method to assess the extent of the loco-regional disease; it is also the best technique to characterize the different components of the lesions [14, 15]. It is clear that MRI has a central place in the diagnosis of AE, while its role in follow-up should be better established in clinical practice [16, 17].

Kodama et al. [16] offered in 2003 a morphological classification scheme of MR findings of AE in the liver based on the different components of the lesions, and as they suggested, MR images may provide some insight into the disease pathophysiology. However, no correlation with the metabolic activity (usually assessed by PET/CT) had been performed to support this hypothesis.

MRI, as non-irradiant and non-invasive follow-up technique, could lower radiation exposure by playing a role in the therapeutic decision.

To our knowledge, no previous comparative study between morphological MR aspects and functional images in similar patient groups has been performed up to now.

The aim of our study was to correlate the appearance of AE hepatic lesions in MRI as defined by Kodama et al., to the metabolic activity visualized in PET/CT.

Materials and methods

Patients

This retrospective study was approved by our institutional review board, and the requirement for patient informed consent was waived.

Criteria to be included in this study were patients recorded in the Registry database, with a confirmed AE diagnosis based on imaging, historical, and serological criteria according to World Health Organization-Informal Working Group on Echinococcosis recommendations [4]; prospective follow-up in our reference center between March 2004 and December 2012; and MRI and PET/CT (at 1 and 3 h after FDG-injection) within a time period of 1 year. Among 132 patients (73 men, 59 women, mean age 64.9 years, range 20–90 years) from the Registry database, in 80, no MRI had been performed; in 3/90 patients with MRI, no PET/CT had been performed; in 4/87, the interval between MRI and PET/CT was >1 year; and in 3/84, no delayed PET/CT acquisition had been performed.

Inclusion criteria were thus fulfilled in 42 AE patients, 25 men and 17 women, aged from 20 to 88 years (mean age 62.2 years) (Table 1).

Techniques

MRI

Liver MRI was performed for all patients in a closed cylindrical high field system of 3 T on the same device (Signa HDx; GE Healthcare, Waukesha, WI, USA). Patients were examined in the supine position. Imaging protocols included unenhanced and contrast-enhanced sequences. Unenhanced sequences consisted of a transverse single-shot fast-spin-echo T2-weighted sequence, and transverse T1-weighted with and without fat-suppressed sequences. A dynamic fat-suppressed gradient echo T1-weighted with a three-dimensional (3D) acquisition sequence (liver acquisition with volume acceleration) was performed before and at 30 s, 1 min, 3 min, and 6 min after the intravenous injection of gadoteric acid (Dotarem 0.5 mmol/mL, Guerbet, France) at a dose of 0.1 mmol/kg of body weight and a flow rate of 2 mL/s, followed by a 20 mL saline flush (Table 2).

PET/CT

Imaging studies were performed on a PET/CT scanner (Biograph; Siemens; CTI; Knoxville, TN) and according to the same vesting schedule. All patients fasted at least 6 h before FDG intravenous injection and were hydrated with sugar-free liquids. Blood glucose concentration determined before FDG-injection of all patients were less than 131 mg/dL (mean 94 ± 3, 6 mg/dL); patients with elevated blood glucose levels (>150–200 mg/dL) had their examinations rescheduled and were scanned when their glucose levels were normal. After tracer injection, patients rested on a comfortable chair during the FDG-uptake period. PET imaging was started 60 min after

Table 1. Characteristics of study population

Group	No. of subjects
Total	42
Male patients	25
Female patients	17
Farmers	4
Hunters	3
Unfenced vegetable garden	7
Consumers of wild berries	5
Forester	1
Treatment by BZM	42
Liver resection	2
Liver transplant	2

BZM, benzimidazoles (albendazole or mebendazole)

Table 2. Imaging parameters used to perform MR sequences

	Single-shot fast-spin-echo T2-weighted	T1-weighted	Fat-suppressed T1-weighted	3D LAVA dynamic fat-suppressed gradient echo T1-weighted
Non-enhanced imaging performed	Yes	Yes	Yes	Yes
Contrast-enhanced imaging performed	No	No	No	Yes
Repetition time (ms)	975–1049	250	4.24	3.43
Echo time (ms)	139.39	2.1	1.19	1.61
Flip angle (°)	90	85	12	10
Matrix	512 × 512	512 × 512	256 × 256	512 × 512
Field of view (cm)	(32–40) × (32–40)	(32–40) × (32–40)	(32–40) × (32–40)	(35–42) × (40–45)
Section thickness (mm)	8	8	8	4
Intersection gap (mm)	1	0	0	No
Section orientation	Transverse	Transverse	Transverse	Transverse
Other				Delay after administration of gadoxetic acid 30 s, 60 s, 3 min, and 6 min

LAVA, liver acquisition with volume acceleration; 3D, 3-dimensional

intravenous injection of 4 MBq/kg of body weight of fluoro-deoxyglucose (18F) (Gluscan 600 MBq/mL, Advanced Accelerator Applications, Saint-Genis-Pouilly, France) through an anterior cubital vein. Patients were examined in the supine position. The subsequent 3D PET data acquisition included 7–9 bed positions (3 min per bed position) over the same axial extent, covering head, thorax, abdomen, and pelvis. A delayed acquisition was performed (2 bed positions for the hepatic region; 3 min each) 3 h after FDG-injection. CT (without contrast material) was performed right before acquisition of the PET images with the patient in the same position. The scanning parameters for whole-body CT cranio-caudal scanning were 130 kV, 90 mAs, 5-mm slice thickness, and a pitch of 1.5. The CT data were used for attenuation-correction of PET emission images and lesion localization (reconstructions with a soft tissue algorithm). Images were reconstructed with the standardized 3D-ordered subset expectation maximization iterative reconstruction algorithm for 3D-PET.

Image analysis

For patients with multiple lesions, the largest lesion was selected in order to avoid bias caused by the small size of the lesions (beyond the resolution of PET imaging) that could lead to false-negative PET/CT results. Indeed, small lesions are detected with much less reliability, particularly in organs such as the liver with background physiologic activity [18].

MRI

MR images were interpreted on a picture archiving and communications system workstation (PACS Carestream Health, Inc., 2011, V 11.3.2.0224) that provided multiplanar reformatted images. All MRI were independently interpreted by a specialized gastrointestinal radiologist (15 years of experience in abdominal MR imaging) and two resident physicians (3rd and 4th year of radiology residency). The three observers were blinded with regard to the PET/CT information. All hepatic lesions of AE were divided into five types according to Kodama's MRI classification—type 1: multiple small round cysts without a solid component; type 2: multiple small round cysts with a solid component; type 3: a solid component surrounding large and/or irregular cysts with multiple small round cysts; type 4: a solid component without cysts; and type 5: a large cyst without a solid component. According to Kodama, hyperintensity on T2-weighted MR images that correlated with signal intensity of the cerebrospinal fluid was defined as a cystic component. Other types of signal intensity on T2-weighted images were defined as solid components (including calcifications) [16]. In case of inter-observer disagreement, final decision was based on the majority findings. Number, location, and size of the lesions, the presence of bile ducts dilation, vessels involvement, and pattern of lesions enhancement after injection (none, slight, marked enhancement) were also evaluated and categorized.

PET/CT

All PET/CT scans were interpreted by two nuclear medicine physicians (with, respectively, 10 and 2 years of experience) blinded with regard to the radiologic information. The acquired images were viewed with software that provided multiplanar reformatted images of PET and CT data alone, and fused PET/CT data (Biograph workstation; Siemens; CTI; Knoxville, TN). For PET/CT analysis, attenuation-corrected PET images, CT images, and coregistered PET/CT images were displayed together on a workstation. Semiquantitative analysis was performed with PET images by normalizing the amount of radiotracer in lesions to the injected dose and patient body weight to obtain a maximum standardized uptake value (SUVmax). PET images were analyzed for the presence of focal lesions

with an increased FDG-uptake. For all patients, attenuation-corrected PET images were used. Lesions were interpreted as active if the uptake at the site of the parasitic lesion was higher than the uptake of the surrounding background tissue observed on either the first or the delayed acquisition. The scan was considered negative when no abnormal increased uptake was noted at 1 and 3 h after FDG-injection. In case of inter-observer disagreement, consensus was reached by discussing the findings. The CT data were used to locate the lesions and the calcifications.

Statistical analysis

Inter-observer agreement between the readers was assessed by using Fleiss κ statistics for MRI (for lesions categorization according to Kodama's classification based on T2-weighted images) and Cohen κ for PET/CT. A κ value of 0.0 indicated poor agreement; a value of 0.01–0.20, slight agreement; a value of 0.21–0.40, fair agreement; a value of 0.41–0.60, moderate agreement; a value of 0.61–0.80, good agreement; and a value of 0.81–1.00, excellent agreement. All statistical analyses were performed by using Excel (v 14.0.4761.1000 SP 3; 2010, Microsoft, Redmond Wash).

Results

MRI

Forty-two lesions were counted and the mean diameter of overall evaluated lesions was 6.3 cm (range from 0.6 to 16 cm). Twenty-three were located in the right lobe of the liver, 7 were in the left lobe, and 12 involved both lobes. Intrahepatic dilation of bile ducts was documented in 9 (21.4%) patients (1 type-2, 6 type-3, and 2 type-4 lesions) and the lesions invaded the vessels in 13 (31.0%) patients (2 type-2, 9 type-3, and 2 type-5 lesions): hepatic veins were involved in nine patients, and for three patients, both hepatic veins and the main portal vein were invaded; the inferior vena cava was invaded in two patients.

Kodama's MRI classification

One lesion (2.4%) was categorized as type 1, 11 (26.2%) as type 2, 24 (57.1%) as type 3, 3 (7.1%) as type 4, and 3 (7.1%) as type 5.

The inter-observer analysis for classification of lesions found a κ coefficient of 0.96.

Pattern of lesion enhancement

In 36/42 patients, no enhancement was observed. In 6/42 (14.3%) patients (3 type-2 and 3 type-3 lesions), a slight enhancement was observed at 3 and 6 min after injection; the enhancement was located at the periphery of the lesions and did not involve their entire rim; the enhancement was mainly located in areas of inhomogeneous low T2-signal intensity and did not correlate with the distribution of the microcystic components.

PET/CT

CT data. Calcifications were detected at CT in 36 patients (85.7%): 8 type-2, 22 type-3, 3 type-4, and 3 type-5 lesions.

Metabolic patterns (Table 3)

At 1 h. Focally increased FDG-uptake in the parasitic liver lesions was observed in all type-1 (n = 1), 63.6% of type-2 (n = 7), and 70.8% of type-3 lesions (n = 17), SUV ranged from 5.6 to 8.5 (mean 6.9).

The inter-observer analysis at 1 h found a κ coefficient of 0.95.

At 3 h. In all type-1 (n = 1), 90.9% of type-2 (n = 10) and 87.5% of type-3 lesions (n = 21) increased FDG-uptake were noted on PET/CT images, and SUV ranged from 5.2 to 9.3 (mean 7.1).

In 1 type-2 (8.1%) and 3 type-3 lesions (12.5%), and all type-4 (n = 3) and 5 (n = 3) lesions, no abnormal increased FDG-uptake was observed on all acquisitions. The inter-observer analysis at 3 h found a κ coefficient of 0.87.

The inter-observer analysis at 1 and 3 h found a κ coefficient of 0.92.

Foci of increased FDG-uptake were located in the periphery of the parasitic lesions (perilesional uptake)on both the early and the delayed acquisition and never involved their entire rim nor their central part; in 25/32 metabolically active AE lesions (78.1%), the increased

Table 3. Correlation between MRI classification of alveolar echinococcosis hepatic lesions as proposed by Kodama to the metabolic activity visualized in 18F-FDG-PET/CT

Lesion type in MRI	No. of lesions	Increased uptake of 18F-FDG in PET-CT at 1 h after radiotracer injection: no. of lesions	Uptake 18F-FDG in PET-CT at 3 h after radiotracer injection: no. of lesions	Total of increased uptake of 18F-FDG (%)
Type 1	1 (2.4%)	1 (100%)	1 (100%)	1 (100%)
Type 2	11 (26.2%)	7 (63.6%)	10 (90.9%)	10 (90.9%)
Type 3	24 (57.1%)	17 (70.8%)	21 (87.5%)	21 (87.5%)
Type 4	3 (7.1%)	0 (0.0%)	0 (0.0%)	0 (0.0%)
Type 5	3 (7.1%)	0 (0.0%)	0 (0.0%)	0 (0.0%)

uptake was observed on more than 50% of the rim; in 7/32 AE metabolically active lesions (21.9%), the increased uptake involved less than 50% of the periphery. There was no significant difference in the extent between the first and the delayed acquisition in metabolically active AE lesions.

Among the 36 lesions with calcifications, 29 (80.6%) were metabolically active and there was not any correlation between foci of increased FDG-uptake and calcifications' distribution.

Correlation between FDG-uptake and morphological MRI appearance (Fig. 1)

A majority of the lesions composed of small round cysts on MRI (1 type-1, 10 type-2, and 21 type-3) had a conspicuous increased FDG-uptake which was located at the periphery of the lesions and foci of increased uptake did not involve the part of the lesions where microcysts were the most numerous. Some of these lesions (1 type-1, 6 type-2, and 14 type-3) had a large photopenic center with a rim of marked FDG-uptake, and the photopenic area corresponded on MR images to areas of cystic components.

All type-5 lesions, which are made of a large cyst without a solid component, were totally photopenic at PET/CT and no peripheral metabolic activity was observed.

Areas of inhomogeneous low T2-signal intensity on MR images demonstrated an uptake equivalent to the uptake of the surrounding background tissue at PET/CT in 2/3 type-4 lesions.

In 5/6 patients (3 type-2 and 2 type-3 lesions) with enhancement after gadolinium injection, foci of increased FDG-uptake were observed.

Among the 42 included patients, three of them had multiple lesions: 2/3 patients had two lesions with a maximal diameter of 0.5 and 8.6 cm for one patient and 0.4 and 5.2 cm for the other one. 1/3 patient had three lesions of 0.4, 0.6, and 7.8 in diameter. None of those infracentimetric lesions were visible on FDG-PET/CT; and only the largest lesion has been considered in order to avoid bias caused by the small size of the lesions.

Discussion

The results of our investigations illustrate that all type-1 and a majority of type-2 (90.9%) and type-3 (87.5%) lesions presented an increased perilesional FDG-uptake on PET/CT images. The relevant part of this observation is that these three different types of AE lesions share a similar MRI characteristic, according to Kodama's MRI classification: indeed, they are all composed of multiple small cysts gathered into "bunch of grapes" or a "honeycomb-like" pattern at the periphery of the lesion [17, 19]. Previous studies suggested that type 1–3 lesions would actually be the early stages of the disease and that the small cysts would directly reflect those infracentimetric parasitic vesicles, characteristic of the development of the metacestode *E. multilocularis* [16, 17, 19]. The metacestode (larva), which consists of the germinal layer, forms small vesicles filled (or not) with protoscoleces, the fertile forms of the larva; these vesicles are surrounded by a granulomatous tissue corresponding to the host's inflammatory immune response which consists, from the center to the periphery, of epithelial cells surrounding the vesicles: macrophages, fibroblasts, myofibroblasts, eosinophils, and various acellular components of fibrosis, then of lymphocytes [20].

The increased FDG-uptake located around parasitic lesions seems rather to be due to this inflammatory immune reaction that occurs randomly around "active" lesions than to the parasite itself [10]; it is thus only an indirect assessment of parasite viability. This explains why there was no predilection for one part of the lesions or the other in the FDG-uptake.

On the other hand, none of the type-4 and type-5 lesions showed an abnormal increased FDG-uptake. In comparison to the types 1–3, they are not made of microcysts but only of solid components including coagulation necrosis and calcifications (type 4) or of a large cavity (type 5) corresponding to a zone of fluid or heterogeneous necrosis, i.e., parasite degeneration [17, 19]. Even though either dilation of the biliary tree or vessels involvement could lead to difficulties in knowing for certain the cause of cystic/necrosis changes, they would not be responsible for the development of microcysts gathered into "bunch of grapes" at the periphery of the lesion. Types 4 and 5 could represent the latest stages of the disease, with very little, if any, parasitic metabolic activity, and thus deprived from any inflammatory reaction: the absence of viable vesicles would lead to the absence of inflammation, and therefore to the absence of metabolically active cells [17, 19, 20].

Four cases categorized as type-2 ($n = 1$) and type-3 ($n = 3$) had no abnormal increased FDG-uptake. Type-3 could be an intermediate stage of the disease, the stage between active (types 1–2) and inactive (types 4–5) AE lesions. The most plausible explanation is a poor inflammatory infiltrate in these lesions.

Among these four patients, one observation supports this hypothesis and may illustrate how MRI combined with PET/CT and serology in the follow-up of patients can assist the therapeutic decision. A 42-year-old woman had a small type-2-lesion of 0.6 cm in diameter, but no increased FDG-uptake was observed on PET/CT images as expected; this apparently paradoxical finding could not only be explained by the size of the lesion: it was too small to be reliably detected by the PET/CT scanner, but is also explained by the immune suppressed status of the patient. Besides, we noticed that she had a negative AE-specific serology; current studies tend to suggest that immuno-

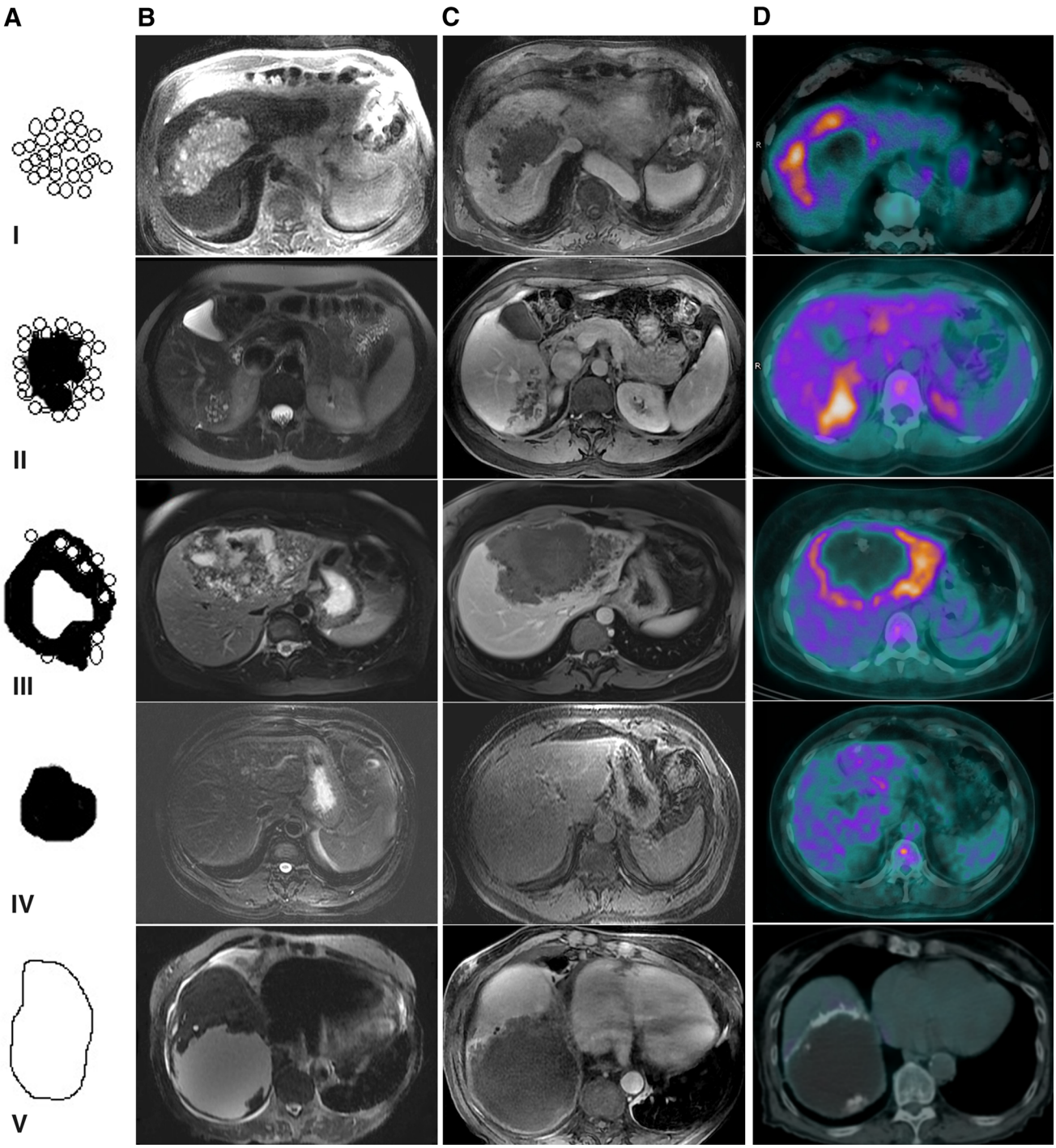

suppression could cause a false-negative serology and PET/CT because of a marked decrease in cells of the immune system that is exactly involved in the periparasitic granuloma. In such cases, disclosure of microcysts on MR images would be a crucial finding to consider the disease still active and postpone treatment withdrawal.

As previously suggested by Reuter et al. [5], no MRI morphological difference was observed in our study between areas of metabolic activity and areas without. Calcifications, which are by far better explored by CT than MRI, were not correlated to areas of increased FDG-uptake; they are only stigmata of a chronic inflammation and their presence has nothing to do with disease activity [5]. As for the enhancement after gadolinium injection, it was slight, and located at the periphery of the lesions (in areas of solid components with low T2-signal intensity) at 3–6 min after injection which means that only the fibrotic or collagenous components were enhanced as already suggested by previous studies [16, 21].

◀ **Fig. 1.** Comparison of MR and PET/CT images in patients with AE liver lesions according to Kodama's MRI classification based on the components of the lesions. **A** Schematic shows the five types of AE liver lesions in Kodama's MRI classification: *type 1* multiple small round cysts without a solid component; *type 2* multiple small round cysts with a solid component; *type 3* a solid component surrounding large and/or irregular cysts with multiple small round cysts; *type 4* a solid component without cysts; *type 5* a large cyst without a solid component. **B** Transverse single-shot fast-spin-echo T2-weighted MR images (repetition time: 975–1049; echo time: 139.39; flip angle: 90) show the five types of AE liver lesions. **C** Transverse fat-suppressed gradient echo-T2-weighted MR images at 1 min after gadoteric acid injection (repetition time: 3.43; echo time: 1.61; flip angle: 10): no enhancement is observed. **D** Transverse PET/CT images at 3 h after FDG-injection: *Id* type 1 lesion, *IId* type 2 lesion, *IIId* type 3 lesion: lesions with peripheral foci of increased FDG-uptake involving only a part of the rim, *IVd* type 4 lesion: solid components without microcysts and no foci I of increased FDG-uptake, *Vd* type 5 lesion: shows a large cyst with peripheral hyper dense calcifications in the right lobe of the liver with no foci of increased FDG-uptake. AE, alveolar echinococcosis.

Microcysts seem thus to be the sole reliable morphological indicator of disease activity; its absence (types 4, 5) could indicate degeneration. Therefore, to prevent patients' irradiation, and especially for those for whom PET/CT is not useful (i.e., in type 4–5 lesions deprived from viable vesicles), MRI could be proposed as a less expensive first-line follow-up examination for the management of AE patients.

The results of this study, in addition to the confirmation they give for the pertinence of Kodama's classification and its usefulness to characterize AE lesions in a standardized manner, highly suggest that MR images also provide some insight into the natural history and functional status of the hepatic lesions. This was demonstrated by the albeit indirect correlation between FDG-uptake at PET/CT, currently considered as the best indicator of lesion progression, and MR images of parasitic vesicles present in types 1–3.

Kodama's classification was not formally recommended by expert groups, not widely used, and had never been evaluated until now. However, we have been able to easily divide all hepatic lesions according to their classification; indeed, it appears that this classification is a simple method to apply and is reliable as well, as the inter-observer analysis, conducted by observers of different levels of experience, found a κ coefficient of 0.96 which correlates to an excellent agreement. It is then clear that this classification is very useful to compare patients' statuses between endemic areas, and in further multicenter studies.

In comparison with Kodama's study, it is evident that our study population is similar to theirs even though our studies took place in two different countries. In addition, even though both are endemic for AE, the studies both took place at different times. Indeed, in their study type-1, type-4, and type-5 were very rare, whereas type-2 and type-3 were the most numerous (Table 4). Hokkaido, Japan, and our region share similar epidemiological characteristics: they both have a high level of health protection, with an organized systematic mass screening of the disease [22, 23].

Our study, however, had several limitations. The first one is the small size of our study population, but AE is a rare disease [1, 2]; since 1982, 509 patients with AE have been diagnosed in France, the country with the highest AE incidence in Europe and among them 188 have been followed in our center. Second of all, we set a relatively short interval of 1 year between PET/CT and MRI. This was explained by the fact that in our predefined schedule, MRI was not systematic but only performed whenever it was justified for diagnosis or therapeutic purposes, as requested by international recommendations [4], and the timing of imaging examinations had not been set to strictly compare them, but to best manage the disease. What is more, the growth and modifications of hepatic lesions between imaging studies are very slow since AE is characterized by an evolution that occurs over many years (between 5 and 15 years) [24, 25]. Another limitation of our study is its retrospective nature; this may have introduced bias in data homogeneity. This disease is common in our region; people who are at greater risk of contracting AE because of their socio-professional environment are subject to a screening by ultrasound [24]. Our study population had mostly a risk of exposure to the parasite and had thus benefited from a screening, which explains why there are a much higher number of types 2 and 3, which are the early stages of the disease, than lesions of type 4 and 5.

Table 4. Comparison of the proportion of each MRI AE hepatic lesion type between Kodama's study and ours

Lesion type according to Kodama's MRI classification	No. of lesions in Kodama's study	No. of lesions in our study
Type 1	2 (4%)	1 (2.4%)
Type 2	20 (40%)	11 (26.2%)
Type 3	23 (46%)	24 (57.1%)
Type 4	2 (4%)	3 (7.1%)
Type 5	3 (6%)	3 (7.1%)

AE, alveolar echinococcosis; MRI, magnetic resonance imaging

Our study demonstrates the need for an additional prospective study and a comparison with histological findings and serology.

In conclusion, this study shows that the presence of microcysts identified by MRI in AE hepatic lesions is correlated to a metabolically active disease. It also confirms the usefulness of Kodama's classification for multicenter studies. MRI can provide non-invasive and non-irradiant information on the metabolic activity of the disease. It can thereby play an important role in the therapeutic decision in order to reduce healthcare costs, the side effects of long-term treatment [4, 26–28], and hence, the quality of life of the patients.

References

1. Kern P, Bardonnet K, Renner E, et al. (2003) European echinococcosis registry: human alveolar echinococcosis Europe, 1982–2000. Emerg Infect Dis 3:343–349
2. Eckert J, Conraths FJ, Tackmann K (2000) Echinococcosis: an emerging or reemerging zoonosis? Int J Parasitol 12–13:1283–1294
3. MiguetJ P, Bresson-Hadni S (1989) Alveolar echinococcosis of the liver. J Hepatol 8:373–379
4. Brunetti E, Kern P, Vuitton DA (2010) Expert consensus for the diagnosis and treatment of cystic and alveolar echinococcosis in humans. Acta Trop 1:1–16
5. Reuter S, Buck A, Manfras B, et al. (2004) Structured treatment interruption in patients with alveolar echinococcosis. Hepatology 39:509–517
6. Wilson JF, Rausch RL, McMahon BJ, Schantz PM (1992) Parasiticidal effect of chemotherapy in alveolar hydatid disease: review of experience with mebendazole and albendazole in Alaskan Eskimos. Clin Infect Dis 15:234–249
7. Ammann RW, Fleiner-Hoffmann A, Grimm F, Eckert J (1998) Long-term mebendazole therapy may be parasitocidal in alveolar echinococcosis. J Hepatol 29:994–998
8. Reuter S, Schirrmeister H, Kratzer W, et al. (1999) Pericystic metabolic activity in alveolar echinococcosis: assessment and follow-up by positron emission tomography. Clin Infect Dis 5:1157–1163
9. Reuter S, Gruner B, Buck AK, et al. (2008) Long-term follow-up of metabolic activity in human alveolar echinococcosis using FDG-PET. Nuklearmedizin 4:147–152
10. Caoduro C, Porot C, Vuitton DA, et al. (2013) The role of delayed 18F-FDG PET imaging in the follow-up of patients with alveolar echinococcosis. J Nucl Med 54:1–6
11. Didier D, Weiler S, Rohmer P, et al. (1985) Hepatic alveolar echinococcosis: correlative US and CT study. Radiology 154:179–186
12. Eckert J, Deplazes P, Kern P (2011) Alveolar echinococcosis (*Echinococcus multicularis*). In: Oxford Medecine (ed) *Oxford textbook of zoonoses: biology, clinical, practice, and public health control*, 2nd edn, Chap. 054. Oxford: Oxford University Press. doi: 10.1093/med/9780198570028.003.0061.
13. Reuter S, Nussle K, Kolokythas O, et al. (2001) Alveolar liver echinococcosis: a comparative study of three imaging techniques. Infection 29:119–125
14. Coskun A, Ozturk M, Karahan OI, et al. (2004) Alveolar echinococcosis of the liver: correlative color Doppler US, CT, and MRI study. Acta Radiol 45:492–498
15. Balci NC, Tunaci A, Semelka RC, et al. (2000) Hepatic alveolar echinococcosis: MRI findings. Magn Reson Imaging 5:537–541
16. Kodama Y, Fujita N, Shimizu T, et al. (2003) Alveolar echinococcosis: MR findings in the liver. Radiology 1:172–177
17. Bresson-Hadni S, Delabrousse E, Blagosklonov O, et al. (2006) Imaging aspects and non-surgical interventional treatment in human alveolar echinococcosis. Parasitol Int 55:267–272
18. Mawlawi O, Podoloff DA, Kohlmyer S, et al. (2004) Performance characteristics of a newly developed PET/CT scanner using NEMA standards in 2D and 3D modes. J Nucl Med 45(10):1734–1742
19. Claudon M, Bessieres M, Regent D, et al. (1990) Alveolar echinococcosis of the liver: MR findings. J Comput Assist Tomogr 4:608–614
20. Hemphill A, Stettler M, Walker M, et al. (2003) In vitro culture of *Echinococcus multilocularis* and *Echinococcus vogeli* metacestodes: studies on the host–parasite interface. Acta Trop 85:145–155
21. Kantarci M, Bayraktutan U, Karabulut N, et al. (2012) Alveolar echinococcosis: spectrum of findings at cross-sectional imaging. RadioGraphics 32:2053–2070
22. Bresson-Hadni S, Laplante JJ, Lenys D, et al. (1994) Seroepidemiologic screening of *Echinococcus multicularis* infection in a European area endemic for alveolar echinococcosis. Am J Trop Med Hyg 51:837–846
23. Wang J, Xing Y, Ren B, et al. (2011) Alveolar echinococcosis: correlation of imaging type with PNM stage and diameter of lesions. Chin Med J (Engl) 124:2824–2828
24. Bresson-Hadni S, Beurton I, Bartholomot B, et al. (1998) Alveolar echinococcosis. Hepatology 5:1453–1456
25. Kadry Z, Renner EC, Bachmann LM, et al. (2005) Evaluation of treatment and longterm followup in patients with hepatic alveolar echinococcosis. Br J Surg 92:1110–1116
26. Grover JK, Vats V, Uppal G, Yadav S (2001) Anthelmintics: a review. Trop Gastroenterol 4:180–189
27. Torgerson PR, Macpherson CN (2011) The socioeconomic burden of parasitic zoonoses: global trends. Vet Parasitol 1:79–95
28. Torgerson PR, Schweiger A, Deplazes P, et al. (2008) Alveolar echinococcosis: from a deadly disease to a well-controlled infection—relative survival and economic analysis in Switzerland over the last 35 years. J Hepatol 49:72–77